AGU PUBLICATIONS

Water Resources Research

RESEARCH ARTICLE

10.1002/2016WR019959

Key Points:
- Quantifying improvements to flood frequency analysis with addition of paleoflood and historical information
- Sensitive analysis to evaluate effects of changing cross sections on paleoflood magnitude reconstruction
- Use of slack-water deposits in semialluvial setting for paleoflood reconstruction

Supporting Information:
- Supporting Information S1

Correspondence to:
D. Lam,
r.lam@uq.edu.au

Citation:
Lam, D., C. Thompson, J. Croke, A. Sharma, and M. Macklin (2017), Reducing uncertainty with flood frequency analysis: The contribution of paleoflood and historical flood information, *Water Resour. Res.*, *53*, 2312–2327, doi:10.1002/2016WR019959.

Received 17 OCT 2016
Accepted 24 FEB 2017
Accepted article online 2 MAR 2017
Published online 22 MAR 2017

Reducing uncertainty with flood frequency analysis: The contribution of paleoflood and historical flood information

Daryl Lam[1], Chris Thompson[1], Jacky Croke[1,2], Ashneel Sharma[2], and Mark Macklin[3,4]

[1]School of Geography Planning Environmental Management, University of Queensland, Queensland, Australia, [2]Department of Science, Information Technology and Innovation, Queensland Government, Australia, [3]School of Geography and the Lincoln Centre of Water and Planetary Health, University of Lincoln, Lincoln, UK, [4]Innovative River Solutions, Institute of Agriculture and Environment, Massey University, Palmerston North, New Zealand

Abstract Using a combination of stream gauge, historical, and paleoflood records to extend extreme flood records has proven to be useful in improving flood frequency analysis (FFA). The approach has typically been applied in localities with long historical records and/or suitable river settings for paleoflood reconstruction from slack-water deposits (SWDs). However, many regions around the world have neither extensive historical information nor bedrock gorges suitable for SWDs preservation and paleoflood reconstruction. This study from subtropical Australia demonstrates that confined, semialluvial channels such as macrochannels provide relatively stable boundaries over the 1000–2000 year time period and the preserved SWDs enabled paleoflood reconstruction and their incorporation into FFA. FFA for three sites in subtropical Australia with the integration of historical and paleoflood data using Bayesian Inference methods showed a significant reduction in uncertainty associated with the estimated discharge of a flood quantile. Uncertainty associated with estimated discharge for the 1% Annual Exceedance Probability (AEP) flood is reduced by more than 50%. In addition, sensitivity analysis of possible within-channel boundary changes shows that FFA is not significantly affected by any associated changes in channel capacity. Therefore, a greater range of channel types may be used for reliable paleoflood reconstruction by evaluating the stability of inset alluvial units, thereby increasing the quantity of temporal data available for FFA. The reduction in uncertainty, particularly in the prediction of the $\leq$1% AEP design flood, will improve flood risk planning and management in regions with limited temporal flood data.

1. Introduction

Globally, floods impacted 2.3 billion people in the last 20 years (1995–2014) and the average number of floods increased by more than 33% compared to the previous two decades [*Centre for Research on the Epidemiology of Disasters*, 2015]. In Australia, numerous extreme floods have been recorded over the past decade with five floods recorded in Southeast Queensland (SEQ) alone. An extreme flood is defined here as any flood at, or above, the ninetieth quantile of the Australia Envelope Curve [*Lam et al.*, 2016]. The extreme floods in 2010–2011 cost the Australian economy ~$30 billion [*Australian Government*, 2015] and resulted in 33 fatalities [*Queensland Floods Commission of Inquiry*, 2012]. Flood risk planning and the use of traditional flood frequency analysis (FFA) to estimate the magnitude of the 1% Annual Exceedance Probability (AEP) design flood is made difficult by short gauging station records. On average, gauging records are 42 years in length for Eastern Australia and many have a poor representation of extreme floods.

Historical flood information and paleoflood records can supplement systematic gauge records to improve at-site FFA, but unlike gauge records, they are noncontinuous and are typically described in terms of above, or below, a flood threshold [*Swain et al.*, 2004]. Historical flood information, which can be derived from flood marks on old buildings, newspaper reports, and oral descriptions [*Herget and Meurs*, 2010], is well documented in Europe with records dating back to A.D. 1500 [*Brázdil et al.*, 2006] and is now being incorporated into FFA [e.g., *Benito et al.*, 2015; *Machado et al.*, 2015]. However, in localities where European settlement occurred relatively recently, such as in Australia, historical flood information has limited capacity to extend the analysis period for FFA.

Table 1. Selected Paleoflood Records in Australia

S/N	River	Setting	Paleoflood Records	Dating Technique	Source
1	Katherine	Bedrock gorge	3	^{14}C	*Baker and Pickup* [1987]
2	Finke	Bedrock gorge	7	^{14}C	*Pickup et al.* [1988] *Wohl et al.* [1994b]
3	Lennard	Bedrock gorge	5	TL, ^{14}C	*Gillieson et al.* [1991]
4	Herbert	Bedrock gorge	6	^{14}C, boulder	*Wohl* [1992]
5	Burdekin	Bedrock gorge	7	^{14}C	*Wohl* [1992]
6	Nepean	Bedrock gorge	1	^{14}C, mineralogy	*Saynor and Erskine* [1993]
7	Fitzroy and Margaret	Bedrock gorge	6, 13	^{14}C	*Wohl et al.* [1994a]
8	Wollombi Brook	Bedrock confined	3	^{14}C	*Erskine and Peacock* [2002]

In contrast, paleoflood hydrology can construct flood magnitudes that occurred 100s to 1000s of years prior to human observation or direct measurement [*Baker*, 1987, 2008]. The method utilizes geological, geomorphological, hydrological, and biological indicators to reconstruct flood peak discharge. The frequently used paleostage indicator (PSI) to reconstruct paleoflood minimum magnitude is slack-water deposits (SWDs) [*Baker*, 2008]. The method requires evidence of deposition of fluvial sediments in low energy zones to enable a minimum stage height for deposition to be determined. Dating the time of deposition provides an indication of the timing of floods which exceed this threshold, although other studies have shown that SWDs may indicate the actual flood height [e.g., *Jarrett and England*, 2002]. Additional information from paleostage indicators (PSIs), such as high water-stage marks which include scarring of tree trunks and silt lines [*Baker*, 1987] helps improve the calibration of hydraulic models used to estimate paleoflood magnitudes.

The global distribution of SWD-PSI studies [*Benito and Díez-Herrero*, 2015] illustrates the wealth of paleoflood archives in North America and Europe. More than 700 radiocarbon (^{14}C)-dated flood records are available in Southwestern U.S. [*Harden et al*., 2010] and projects such as SPHERE (Systematic, Paleoflood and Historical data for improvEment of flood Risk Estimation) [*Benito et al*., 2004] have led to the compilation of extensive ^{14}C flood databases in Europe [e.g., *Macklin and Lewin*, 2003; *Thorndycraft and Benito*, 2006]. However, there are few Australian paleoflood studies (Table 1, Figure 1) and only two have attempted to integrate their reconstructed paleoflood data into FFA [*Baker and Pickup*, 1987; *Wohl et al*., 1994b].

Recent advances in dating flood sediments using single-grain Optically Stimulated Luminescence (OSL) and statistical age models are also providing greater insights into past flood activity with improved accuracy [e.g., *Croke et al*., 2016]. Despite these advances, two main limitations to the application of paleoflood records remain. The first is the lack of suitable sites. Bedrock gorges are the preferred setting for the reconstruction of paleoflood information from SWDs due to their stable channel boundary condition [*Webb et al*., 2002]. In contrast, alluvial channels are often susceptible to phases of channel erosion and/or deposition leading to uncertainty in estimating changes in channel capacity over time. However, semialluvial reaches in the form of macrochannels exist in Australia [*Croke et al*., 2013], South Africa [*Heritage et al*., 2001], and Central Texas, USA [*Heitmuller et al*., 2015]. Macrochannels have relatively stable boundary conditions confined within Pleistocene terraces and provide the potential to evaluate the preservation of SWDs outside bedrock gorge settings.

The second reason for the limited application is the lack of a consistent methodology for the integration of noncontinuous data with continuous gauging data. The development of the Peak-Over Threshold (POT) method and other Bayesian type models [e.g., *Parkes and Demeritt*, 2016] in recent years is beginning to address this limitation. The main aim of this paper is to improve the estimation of design flood (1% AEP) for at-site FFA by incorporating historical and paleoflood records in SEQ. The specific objectives are as follows:

i. To evaluate the extent of change in semialluvial channel settings for paleoflood reconstruction.
ii. To determine the sensitivity of FFA to changes in channel boundary dimensions.
iii. To apply the methodology to existing paleoflood records across Australia.

2. Study Area

The study region is located in SEQ, Australia (Figure 1), a tectonically stable region with geology dominated by Paleozoic and Mesozoic-Paleozoic age rocks [*Blewett et al*., 2012]. Eleven major drainage basins exist

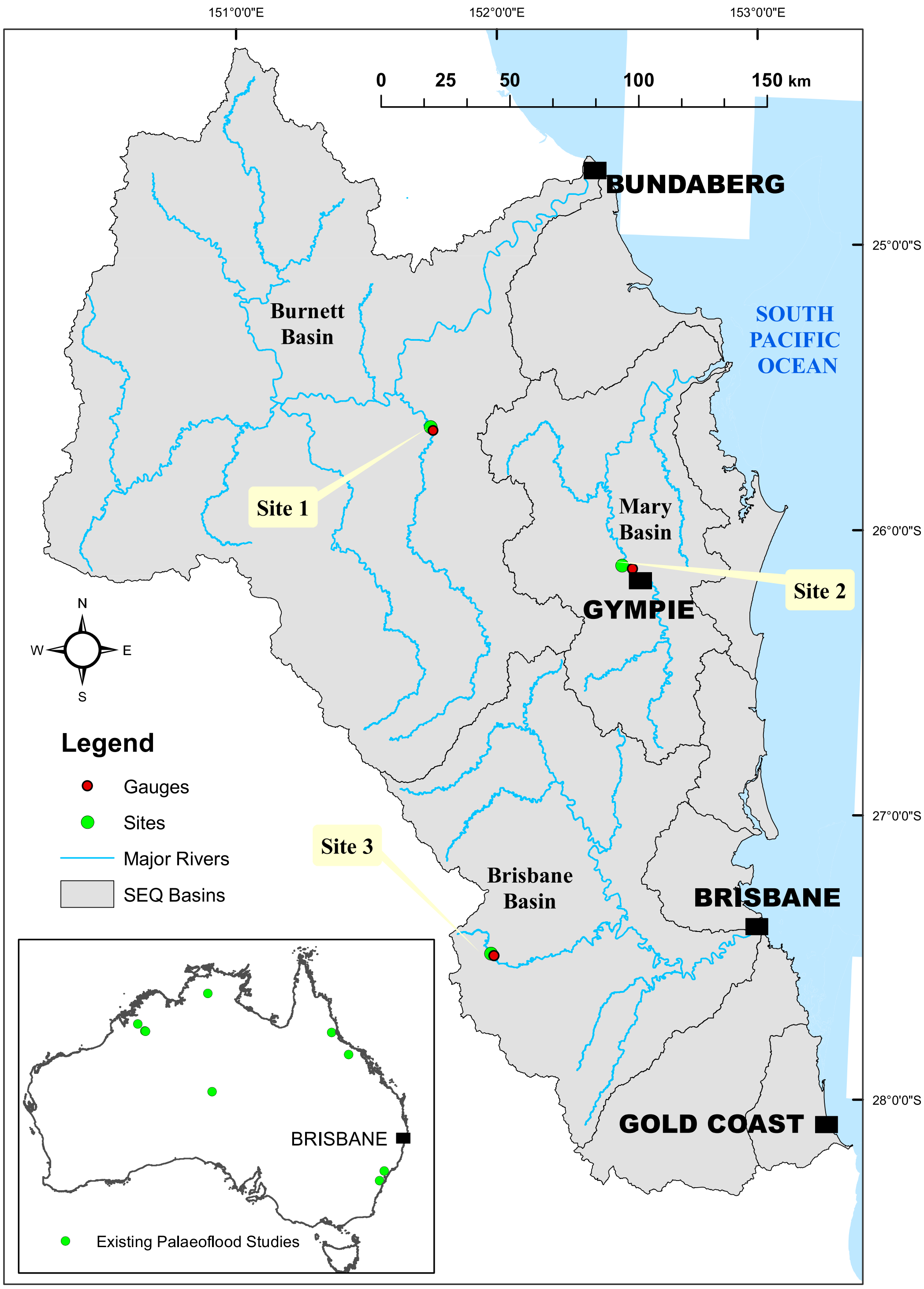

Figure 1. The study region in Australia with the location of sites (1) in the Burnett Basin, (2) in the Mary Basin, and (3) in Lockyer Creek subcatchment of the Brisbane Basin. (Insert) Existing paleoflood records.

throughout SEQ with the Burnett, Mary, and Brisbane representing the largest catchments (Figure 1). The region experiences a subtropical climate with average daily temperature ranges of 6–27°C and mean annual rainfall of between 650 and 2850 mm (Bureau of Meteorology data are available at http://www.bom.gov.au). Notably, the region has very high flood variability based on metrics of the Q_{50}:Q_2 flood quantile ratio and Flash Flood Magnitude Index [*Rustomji et al.*, 2009]. This also highlights the potential effect of the low outliers in annual maximum series (AMS) observations in distorting the AEP of the larger flood quantile [*Lamontagne et al*., 2016]. In Eastern Australia, these Potential Influential Low Flows (PILFs) account for 61% of the difference in the flood quantile estimation in 10 study catchments [*Rahman et al*, 2014].

European settlement in SEQ commenced in 1840s with the establishment of towns such as Brisbane, Gympie, and Bundaberg (Figure 1) which provide the oldest historical flood records. Land use change has occurred since with extensive conversion of native vegetation to agricultural and pastoral lands on the floodplains, while headwater catchments remain forested with native vegetation [*Capelin et al*., 1998].

2.1. Study Catchments

Three sites were selected across the three major catchments: the Burnett, Mary, and Brisbane (Figure 1). These are representative of major drainages throughout the region spanning drainage areas of between 9500 and 33,000 km^2 and have mean annual rainfalls of between 650 and 2850 mm.

The first site (Site 1) is located on Barambah Creek in the Burnett Basin (Figure 2a, Table 2). The reach is laterally confined by Barambah Basalts into which the river has progressively incised since the lava flows $\sim$ 600,000 years ago [*Willmott*, 1986]. There are alluvial fill units inset within the main channel. Bedrock bars along the channel are exposed during low flow revealing a thin alluvial cover. The second site (Site 2) is located on the Mary River at Fisherman's Pocket and is located 12 km downstream of the historical gold mining town of Gympie (Figure 2b, Table 2). The selected SWDs sites are located in a laterally confined, constriction reach where the river has incised into the resistant basaltic bedrock of the Gympie Group [*Pointon and Collins*, 2000]. The third site (Site 3) is located on Lockyer Creek, a tributary of the Brisbane River downstream of Wivenhoe Dam (Figure 2c, Table 2). The upstream catchment area was the focal point of the 2011 supercell storm, which generated an extreme flood causing significant in-channel scouring in the upstream reaches [*Sargood et al*., 2015; *Thompson and Croke*, 2013].

Channels in these subtropical catchments are characterized by a macrochannel morphology, a type of channel-in-channel form which can contain floods with ARIs of $>$50 years [*Croke et al*., 2013]. Recent research has shown that these semialluvial channels are laterally stable due primarily to fine-grain-resistant boundary sediments or bedrock, and adjustment is often confined to within the boundary of the macrochannel [*Fryirs et al*., 2015; *Thompson et al*., 2016]. Floodplain and terrace chronological investigations in Lockyer Creek suggest the macrochannel formed and has been locked into its current position, between 2000 and 7000 years [*Croke et al*., 2016; *Daley et al*., 2017].

3. Methods

Sites from the Burnett, Mary, and Lockyer catchments were selected for slack-water investigation based on the following criteria:

i. Located within 10 km of gauging stations and without major intervening tributary to enable hydraulic model calibration for paleoflood reconstruction.
ii. Located in reaches with flow confined by resistant boundary, mainly bedrock, in which all flood flow is contained.
iii. Presence of features that promotes slack-water sediment deposition and preservation during flood flows.
iv. Minimal colluvium deposition.

Criteria (i) and (ii) were evaluated by desktop analysis while criteria (iii) and (iv) required field investigation of the slack-water setting and evaluation of the stability of the boundary conditions.

3.1. Selected Field Sites

At each site, a trench or pit was excavated and the soil stratigraphy was documented to include: depth, grain size, lamination, dip direction, bioturbation, and color. These attributes are used to infer the nature of deposition and the minimum paleoflood discharge required for sample deposition. In the Burnett catchment, two slack-water settings along the tributary of Barambah creek were examined. Site 1A is located on the inside of a sharp bend where flow has formed a large scour pool twice as wide as the average channel width (50–100 m), which is protected behind a basalt spur (Figure 2a). A slack-water bench on the inner bend extends approximately 200 m downstream. An additional site (Site 1B) in the backwater zone of a

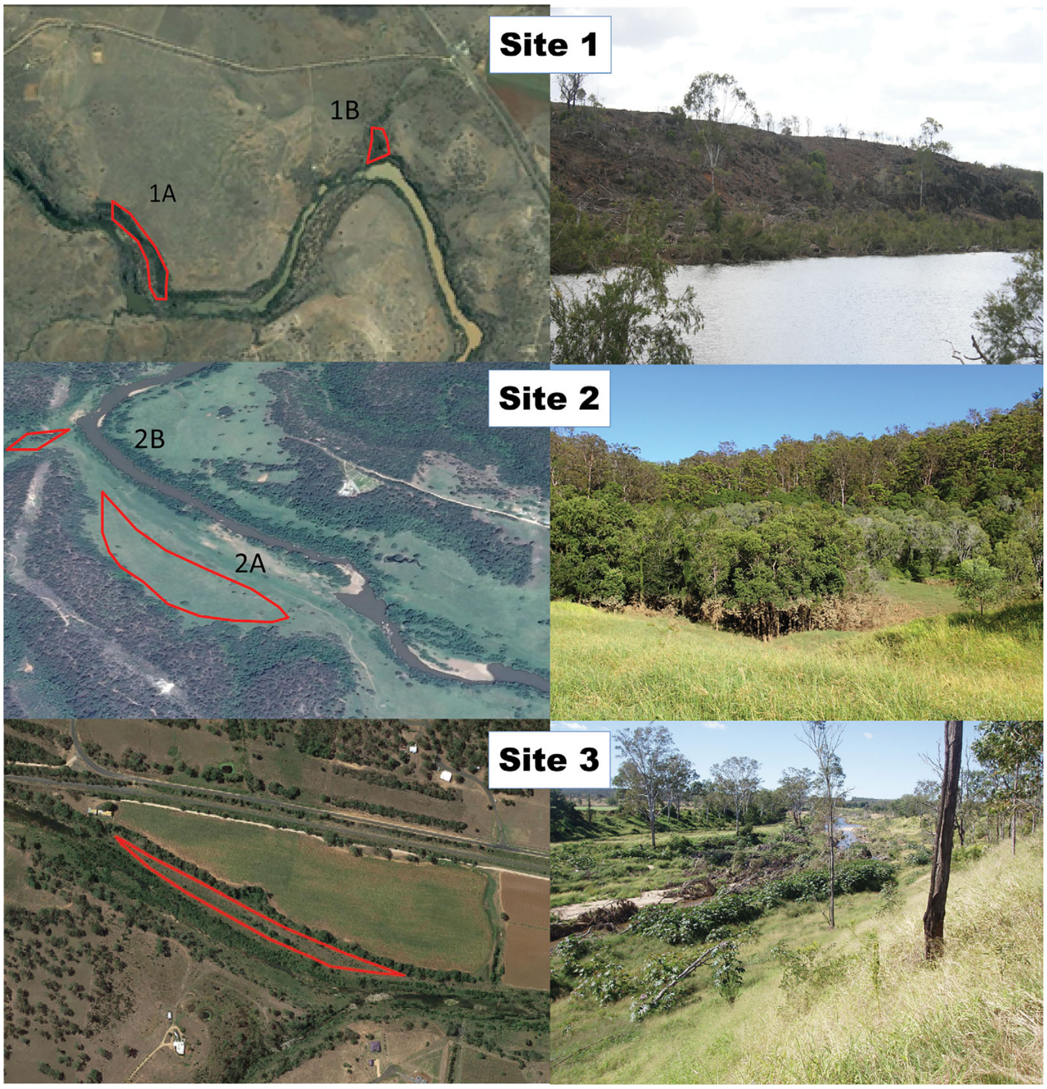

Figure 2. Reach and SWD settings for all three sites. (Site 1) Ban Ban Springs, showing two SWD sites in red polygons, (1A) expansion zone behind lee of spur and (1B) small tributary backwater zone. Flow direction is from right to left. (Photo) Study reach dominated by bedrock outcrops. (Site 2) Fisherman's Pocket, illustrating (2A) expansion zone behind lee of spur and (2B) tributary backwater zones in red polygons. Flow is from bottom right to top left. (Photo) Silt line from 2015 flood used for hydraulic model calibration. (Site 3) Helidon, illustrating an inset floodplain (red polygon) within the macrochannel boundary. Flow is from left to right and the exit of the bend marks the transition from bedrock confined. (Photo) Photo of macrochannel looking downstream with inset floodplain surface on left bank.

tributary confluence is located ~2 km upstream of Site 1A. An extreme flood occurred in 2013 and was the largest recorded in the nearest gauging station (136207A; 1967 to present) located ~2 km upstream (Table 2). A debris line from the 2013 flood was surveyed and used to calibrate the hydraulic model. In addition, known stage heights of the 2013 and 2015 floods were provided by land owners for model calibration.

Table 2. Reach and Gauging Station Information

	Site 1	Site 2	Site 3
River Catchment	Burnett River	Mary River	Brisbane River
River/Creek name	Barambah Creek	Mary River	Lockyer Creek
Site/reach name	Ban Ban Springs	Fisherman's Pocket	Helidon
Contributing area (km^2)	5556	3095	357
Nearest gauging stations	136207A (2 km upstream)	138007A (3.5 km upstream); 138020A (discontinued) (9.5 km upstream); 040776 (discontinued); and 040993 (9.0 km upstream)	143203A,B,C (1.3 km downstream)
Gauge start year	1966	1910	1926
Gauge length (years)	49	106	88

Two slack-water settings were examined along a 1.5 km reach in the Mary catchment. Alluvial fill along the reach is exemplified by a bench within the macrochannel. Site 2A (Figure 2) is an expansion zone behind the lee of a spur and Site 2B is on the upstream side of a tributary confluence. A prominent silt line from the 2015 flood (tenth largest on record) was surveyed for hydraulic calibration of stage height with the upstream gauging stations (Figure 2, Table 2). The landowner provided elevations of the 2013 flood stage height (fourth largest on record), which was also used for hydraulic model calibration and paleoflood reconstruction.

Site 3 on the upper mid reaches of Lockyer Creek is located within a highly resistant and laterally stable reach of the river. Negligible channel change has occurred along this reach during recent extreme floods and throughout historical timescales [*Fryirs et al*., 2015] due to the resistance of the confining terrace material [*Daley et al*., 2017]. The setting is a discontinuous floodplain unit set within the confining terrace in a channel expansion zone [*Croke et al*., 2013].

3.2. Age Dating

Sediment samples were collected from each mapped flood unit for OSL dating and carbon materials are collected for ^{14}C dating. The OSL samples were processed following procedures outlined in *Aitken* [1998]. Single-grain equivalent dose (D_e) values were determined using the modified single aliquot-regenerative dose (SAR) protocol of *Olley et al*. [2004] in combination with the acceptance/rejection criteria provided in *Pietsch* [2009]. A burial dose (D_b) from each population of single-grain D_e values was calculated using the age modeling approach of Galbraith and coworkers [*Galbraith and Laslett*, 1993; *Galbraith et al*., 1999; *Roberts et al*., 2000]. ^{14}C dating was used to supplement OSL dating. The carbon materials collected were analyzed with Accelerated Mass Spectrometry ^{14}C dating by Beta Analytic, following standard methods. The conventional age was calculated after *Talma and Vogel* [1993]. The calibration to calendar years was carried out using the SHCAL13 database [*Hogg et al*., 2013].

OSL and ^{14}C dates are reported as a central age ± 1 and ± 2 sigma errors, respectively. SWDs within error in the same reach are deemed as potentially the same flood and a pool mean age is used to prevent overlapping periods in the FFA (see section 3.3).

Paleoflood discharges based on SWDs with ages beyond the last $\sim$1000 years are not considered in the FFA. This is to avoid the effects of potential changes in the hydrological regime as a result of shifting climate regime. A significant change in climate has implications for hydrological conditions in terms of catchment antecedent moisture, rainfall intensity, frequency, and magnitude. The region is believed to have shifted from a dry regime with short wet phases to a regime with frequent wet phases after 1000 cal. year BP [*Woodward et al*., 2014].

3.3. Paleoflood Reconstruction

Minimum flood magnitude for SWD inundation was derived using the one dimensional U.S. Army Corps of Engineers HEC-RAS hydraulic model (http://www.hec.usace.army.mil/) with input data and parameter settings in supporting information Table S1. Cross-section surveys were extended upstream and downstream of each SWD site to minimize the effect of the set boundary conditions on the stage height. The calibrated model is then applied to determine the paleoflood magnitude by iteratively increasing discharge until inundation of the SWD is achieved.

3.4. Testing for Stable Boundary Conditions

Geomorphic settings with stable boundaries such as bedrock reduce the likelihood of significant changes to the channel cross sectional between floods. However, if channel boundaries erode or aggrade significantly, then reconstructed paleoflood discharges may be underestimated or overestimated.

To evaluate the stability of the macrochannel boundary for potential cross-sectional change, additional trenches were excavated in the inset units to enable investigation of possible erosional contact layers, the depositional age, and depth of sediment underlying a SWD deposit. The age and depth of sediment collected at various depths (i.e., upper and lower geomorphic units) also enabled the calculation of sediment deposition/accretion rates to determine potential changes in channel capacity since emplacement of the SWD. A uniform rate of deposition along the study reach is assumed. The respective accretion rates are applied to the time length since the oldest recorded paleoflood deposition at the site. The depth of

Table 3. Peak Stage Height of Major Floods in Gympie, Mary River[a]

Year	Date	Time	Record Type	BoM Station 040993 Height (m)	Fisherman's Pocket Station 138007A Height (m)
1870	11 Mar 1870		Historical	21.59	22.72[b]
1889	29 Jul 1889		Historical	16.92	18.18[b]
1890	25 Jan 1890		Historical	19.28	20.47[b]
1893	4 Feb 1893	0300	Historical	25.45	26.48[b]
1898	11 Jan 1898	2300	Historical	22.00	23.12[b]
1955	28 Mar 1955	1730	Gauge	21.44	22.58
1973	9 Jul 1973	0200	Gauge	19.61	20.80
1974	28 Jan 1974	0500	Gauge	20.73	21.89
1989	3 Apr 1989	2130	Gauge	19.65	20.83
1992	22 Feb 1992	2100	Gauge	21.4	22.54
1999	10 Feb 1999	0400	Gauge	21.95	23.07
2011	11 Jan 2011	0500	Gauge	19.45	20.64
2013	28 Jan 2013	1210	Gauge	19.98	21.16

[a]Historical data provided by BoM.
[b]Calibrated stage height.

sediment is then removed from the geomorphic unit within the macrochannel. These adjusted cross sections based on estimated cross-sectional area changes are used to compare the effects of potential boundary condition changes.

3.5. Including Available Historical Records

Verifiable historical flood records were only available from the gold mining town of Gympie located near the Fisherman's Pocket site (Site 2) in the Mary River catchment (Figure 2). For the other sites, early settlement towns were located too far away to provide reliable historical flood information. Historical observations of major floods from Gympie extend back to the 1870s (Table 3) and the records consist of marked flood heights on buildings, bridges, and power poles. The stage height marks have been calibrated to flood height and magnitude at the Bureau of Meteorology (BoM) gauging station (040993) located 9.0 km upstream of Site 2 at Kidd Bridge, Gympie (Figure 2). The records were then converted to stage heights at the Fisherman's Pocket station (138007A) which is ~3.5 km upstream. This was achieved by producing a cross-correlation linear equation between all available gauged daily peak stage heights (1998–2005) from the Gympie station (138020A) and Fisherman's Pocket station (supporting information Figure S1).

3.6. Flood Frequency Analysis With Bayesian Inference Method

The FFA was computed using Bayesian Inference in the FLIKE software [*Kuczera*, 1999]. The Bayesian Inference methodology allows for (i) the integration of records outside the gauge period and (ii) data to be censored with the use of minimum/maximum discharge thresholds (http://flike.tuflow.com). Historical and paleoflood data are added individually as a flood that occurred within a given time block. Each of these is an added censored data and there is no overlap in the time block for each of the censored data range.

OSL/^{14}C age range is first converted to A.D. years which provides the start and end year of the time block. The threshold value used here is the estimated discharge value ($m^3\ s^{-1}$) of the historical/paleoflood data. Set as a minimum threshold value, this censors the rest of the years within the time period, i.e., a discharge of this magnitude has only occurred once within this period/time block. The minimum discharges are minimum threshold values because historical data are traditionally done by visual recording and may not necessarily represent the peak stage height. Minimal threshold is also used for estimating discharges of a paleoflood since the reconstructed discharge is derived from the minimum stage discharge required to inundate the surface.

Five probability distribution models (lognormal (LN), Log Pearson type III (LPIII), Gumbel, Generalized Extreme Value (GEV), and Generalized Pareto (GPA)) were considered for each site. The selected model was based on the goodness of fit of all data within the 90% confidence limits and the standard deviation of $\log_{10}$ discharge for the 1% AEP.

The Multiple Grubbs and Beck (MGB) test was performed to evaluate probable effects of PILFs in the AMS. The evaluation of the change in uncertainty was based on the range of the 90% probability limit of the 1% AEP quantile. An increase in range was interpreted as an increase in the uncertainty and vice versa.

4. Results

4.1. Slack-Water Deposits and Channel Boundary Identification

The relative elevation of the SWDs to the channel and the site stratigraphic profiles are shown in Figure 3. Sampled SWDs range in size from silt to fine sand and typically were found overlying compacted and older deposits as demarcated by some paleosol development. The stratigraphy consisted of predominantly

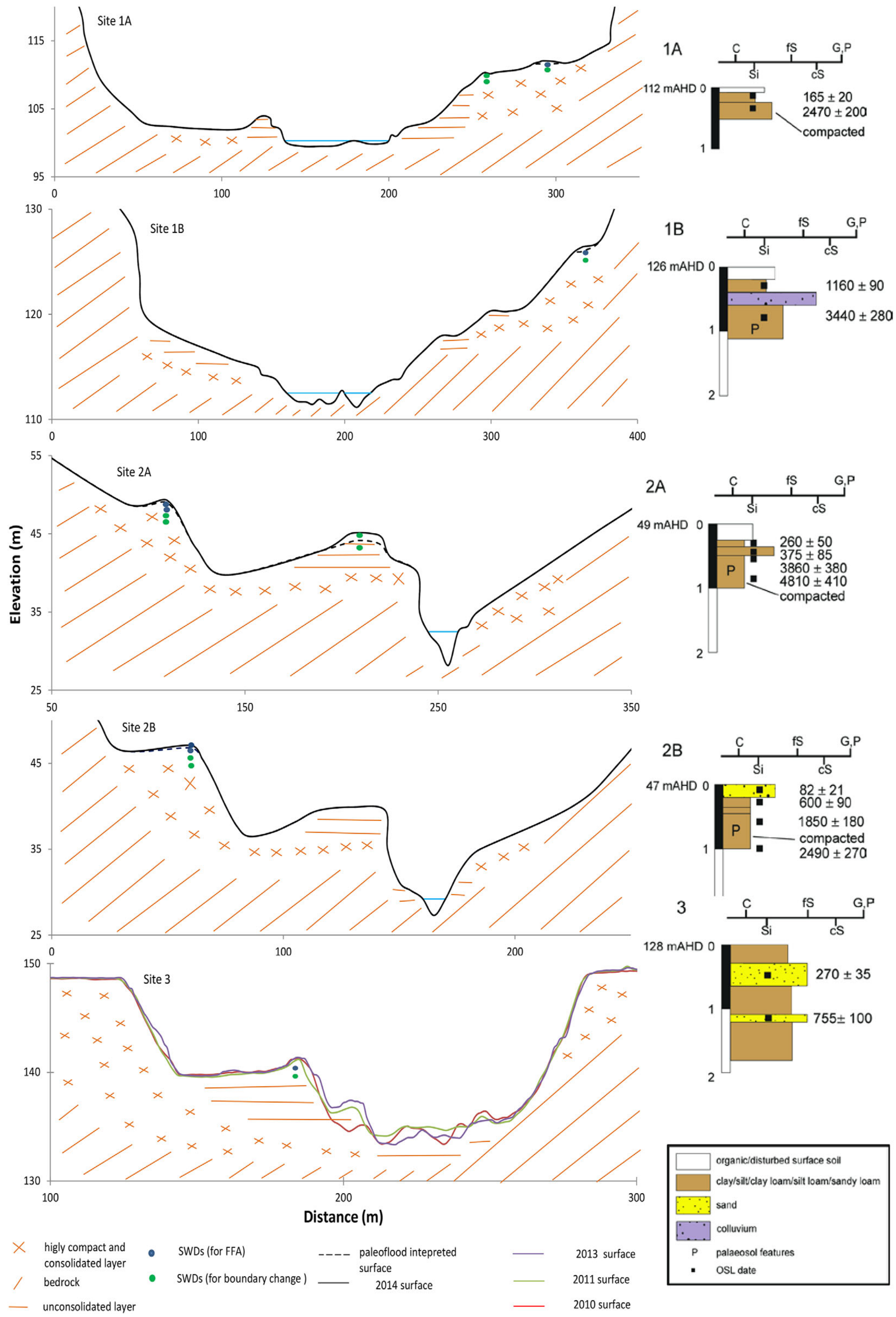

Figure 3. Representative channel cross sections showing SWDs locations and boundary conditions.

horizontally bedded units, which were gradational and showed no distinct erosional contacts between units. There was a notable unit change between the upper, younger SDWs and the basal, older compacted units which showed some paleosol development. A more detailed summary of the SWDs stratigraphy is provided in Table 4.

Table 4. Summary of SWD Stratigraphic Descriptions

SWD Unit	Thickness (m)	Grain Size	Lamination	Dip	Bioturbation	Boundary Condition to Lower Unit	Color	Remarks
1A1	0.17	Fine to coarse silty loam	No distinct lamination	5° dip away from channel	Minor	Distinct (sharp reversal in grain size, compacted unit below)	10YR3/4	Lens-shaped (levee) feature pinches away and downstream to channel
1B1	0.19	Fine silty loam to very fine sand	Poor lamination	Nil	Few roots	Distinct (colluvium boulder deposit)	10YR3/4	Paleosol development in unit below
2A1	0.1	Clay loam	No distinct lamination	<5° dip away from channel	Few roots	Poor (bioturbation, consolidated unit below)	10YR5/6	Some charcoal staining, more compact than unit below (2A2)
2A2	0.15	Silty-clay loam	Poor lamination	<5° dip away from channel	Nil	Distinct (color, grain size, compacted unit below)	10YR4/6	Sitting above a very compact clay loam layer (>0.5 m)
2B2	0.15	Silty-clay loam	Poor lamination	Nil	2 cm diameter horizontal root at the top boundary	Distinct (palesol development)	7.5YR5/8	Sitting above a thick clay loam compacted layer (>0.4 m), with no laminations but occasional rounded sand and pebbles
3A1	0.2	Fine sand	No distinct lamination	Nil	Minor, few small roots	Distinct (Paleosol)	2.5Y8/2	Sitting above a 50 cm dark brown loam layer

4.1.1. SWD Chronology

All SWDs samples included quartz, which proved suitable for single-grain OSL dating with recovery ratios (the number of grains accepted versus the number of grains analyzed) of 10 ± 5%. The majority of samples showed high overdispersion (>20%) consistent with partial bleaching, hence these were analyzed using the minimum age model (MAM). The remaining samples were analyzed using the central age model (CAM). The age and depth of the six SWDs range from 165 ± 20 to 1160 ± 90 OSL years (Table 5). The age of the SWD at Site 1B (1160 ± 90) is just more than 1000 years and is also included in the FFA.

4.1.2. Channel Adjustment Based on SWD Elevations and Ages

Twelve additional sample ages and depths are used to determine changes in the channel boundary at the time of the paleoflood and post-paleoflood aggradation (Table 5, Figure 3). These confirm that the SWD overlies much older (>1000 years) surfaces (Table 5) and that within-channel aggradation rates range between 0.04 and 8.75 mm a^{-1} (Table 6).

Table 5. Summary of SWDs and Other Geomorphic Units' Depth and Ages

Site	Unit ID	SW Setting	Depth (m)	Ages (Years)
1A	1A1	Expansion zone behind lee of spur	0.24	165 ± 20
1B	1B1	Tributary mouth	0.4	1160 ± 90
2A	2A1	Expansion zone behind lee of spur	0.35	260 ± 50
	2A2	Expansion zone behind lee of spur	0.52	375 ± 85
2B	2B2	Tributary mouth	0.35	600 ± 90
3	3A1	Expansion zone	0.3	270 ± 35
		Geomorphic Units[a]		
1A	1AA1	Lower geomorphic unit	0.62	1520 ± 120
	1AA2	Lower geomorphic unit	1.08	1830 ± 160
	1A2	Upper geomorphic unit	>0.43	2470 ± 200
1B	1B2		1.10	3440 ± 280
2A	2A3	Upper geomorphic unit	0.6	3860 ± 380
	2A4	Upper geomorphic unit	0.85	4810 ± 410
	2AA1	Lower geomorphic unit	1.00	200 ± 30
	2AA2[b]	Lower geomorphic unit	>2.25	1340 ± 30
2B	2B1[c]		0.15	82 ± 21
	2B3		0.4	1850 ± 180
	2B4		>1.00	4970 ± 30
3	3A2[d]			755 ± 100

[a]The upper and lower geomorphic units are used to differentiate the two pits at different elevations in the same reach.
[b]20 cm depth paleosol between this and the unit above.
[c]SWD excluded from FFA, interpreted as the included 1955 historical flood.
[d]Surveys before and after two largest floods (2011, 2013) showed no significant change.

4.2. Flood Frequency Analysis

Four probability distribution models (GEV, GPA, LPIII, and LN) showed good fit with most data points within the relatively narrow 90% probability limits. The LPIII model provided the best fit for the FFA analysis of the 1% AEP at Sites 1 and 2, while the GEV provided the best fit for Site 3. The standard practice of using a common distribution model that best fits the data for the majority of sites is not appropriate here given the limited number of sites. In addition, the newly revised Australian Rainfall and Runoff (ARR) guidelines note the use of different distributions may be required for different circumstances [*Kuczera and Frank*, 2016]. The 1% AEP is used here to demonstrate the effects of change with the integration of historical and/or paleoflood records. Other % AEPs and the posterior moments are provided in supporting information Table S2.

10.1002/2016WR019959

Table 6. Range of Accretion Rates for Various Sampled Units

Site	Unit	Rate (mm a^{-1})
1A	Lower geomorphic unit	0.18–0.43
1A	Upper geomorphic unit	0.1–0.73
1B		0.2–0.65
2A	Lower geomorphic unit	3–8.75
2A	Upper geomorphic unit	1.15–1.3
2B		0.04–0.12

The MGB Test did not identify any PILFs at Site 1 on Barambah Creek and all records are used to estimate the magnitude of the 1% AEP flood of ~8800 m^3 s^{-1} (Table 7), which equates to a >10% reduction in the estimated discharge of the 1% AEP. More importantly, the inclusion of two paleofloods reduced the uncertainty range of the 1% AEP by 62% (Figure 4a).

The MGB Test excluded 23 outliers for the LPIII probability distribution model for Site 2 on the Mary River. The integration of five historical floods (Table 3) and the addition of three paleofloods reduced the uncertainty range of the 1% AEP by 51% (Figure 4b). The estimated discharge of the 1% AEP flood revised downward (<7%) from 7900 to 7400 m^3 s^{-1} (Table 7).

The MGB Test excluded 20 low outliers from the FFA at Site 3 on the Lockyer Creek. The uncertainty range of the 1% AEP reduced by 54% with the addition of one paleoflood (Figure 4c). The magnitude of 1% AEP flood also reduced significantly (~25%) from 2200 to 1050 m^3 s^{-1} (Table 7).

4.3. Sensitivity Analysis of Changes in Cross-Sectional Area

No erosional contact layers were evident in the SWD stratigraphy, but to evaluate the sensitivity of the paleoflood magnitude estimates to possible erosion since deposition, the aggradation rates of the within-channel features were used to project likely changes in within-channel unit elevation. Inferring from the age and depths of the SWDs and geomorphic units, within-macrochannel depositional features indicate accretion ranging from 0.04 to 8.75 mm a^{-1} (Table 6). This translates to a likely increase in channel cross-section area of between 3.8 and 10.6% and a resultant reduction in the estimated minimum discharge from between 11.1 and 39.2% (Table 8).

Site 1 in Barambah creek showed minimal changes to the estimated discharges despite a reduction in cross-sectional area of more than 10% (Figure 5a). In the case of Site 2 in the Mary catchment, the effect of cross-sectional area changes remains within the 90% confidence limits of the initial FFA for the larger AEPs (Figure 5b). The sensitivity analysis shows minimal effects for the infrequent paleoflood estimation. Despite a reduction in estimated minimum discharges of up to 39% (Table 8) required for inundation of the SWD surface, the effect of small cross-sectional area is reduced through the integration of this additional paleoflood information into FFA.

4.4. Extending the Application to Past Paleoflood Studies in Continental Australia

From the existing data base of paleoflood records in Australia (Table 1), three sites met the criteria as outlined in section 3, and the paleoflood records were integrated with the AMS of the nearest gauging station for FFA (Table 9). These show a reduction in the uncertainty range of the 1% AEP of between 58 and 65% with the addition of one to five paleoflood records (Table 9).

5. Discussion

Floods are a recognized global hazard and in many parts of the world, the ability to accurately project the frequency and magnitude of extreme flood is often severely limited by short gauging records [*Merz and Blöschl*, 2008]. With gauging records routinely less than 50 years and often missing big floods, there is little certainty of projecting the frequency of these floods based on traditional FFA [*Benito et al.*, 2004]. For

Table 7. Summary of Number of PILFs, 1% Annual Exceedance Probability and the Associated 90% Probability Limits for All Three Sites

		Systematic			Systematic + Historical/Paleoflood		
			90% Probability Limits			90% Probability Limits	
Site	PILFs	1%AEP Estimated Discharge (m^3 s^{-1})	Lower (m^3 s^{-1})	Upper (m^3 s^{-1})	1% AEP Estimated Discharge (m^3 s^{-1})	Lower (m^3 s^{-1})	Upper (m^3 s^{-1})
1	0	10,020	3950	37,300	8800	4850	17,480
2	23	7,900	5800	12,450	7400	6050	9,350
3	20	2,200	1150	5,600	1650	1050	3,050

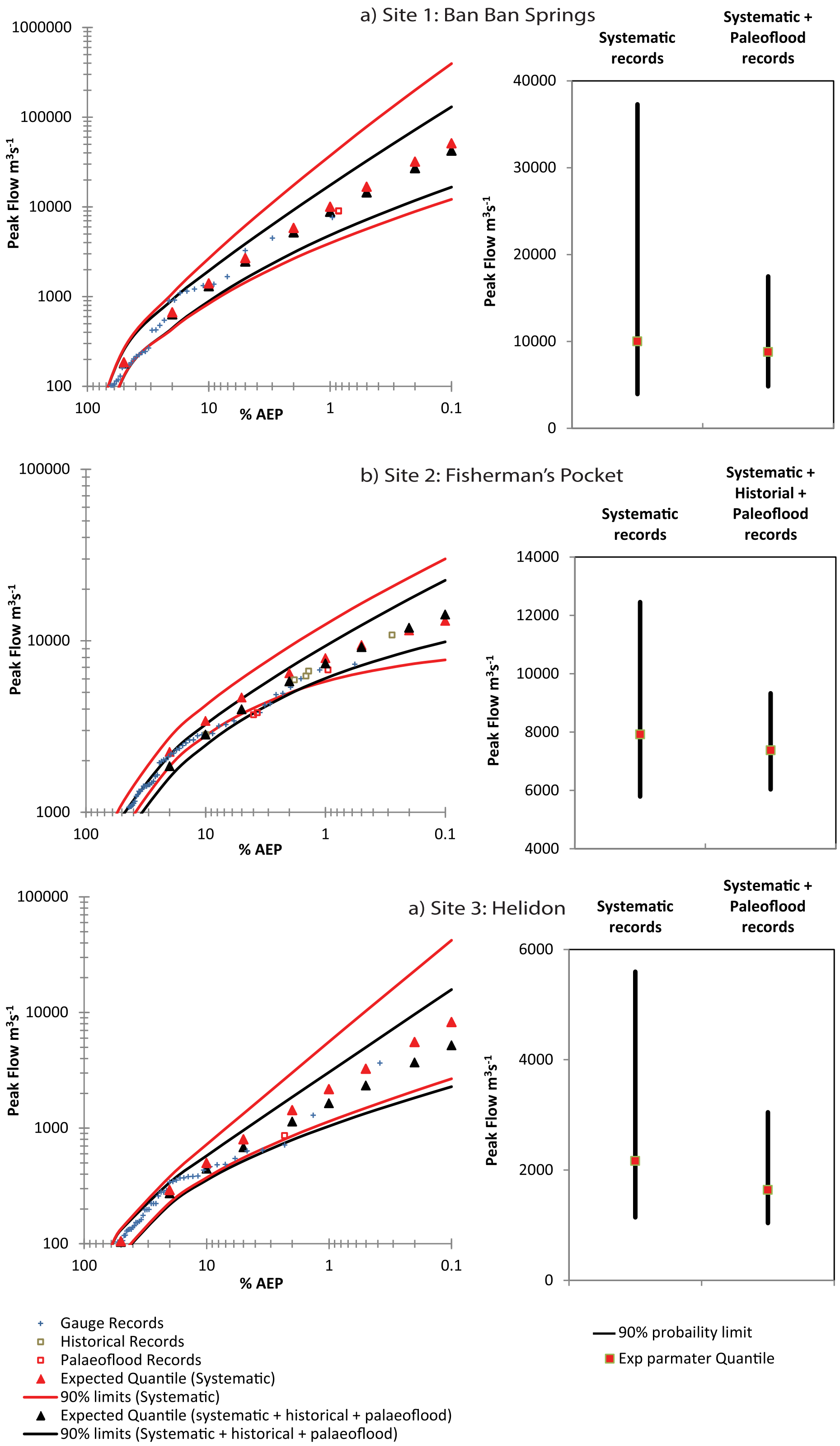

Figure 4. Changes to uncertainty range of estimated quantile based on the 90% probability limit up to the 1% AEP flood. (left) FFA results showing before and after integration of historical and/or paleoflood records. (right) The reduction in uncertainty range for 1% AEP.

Table 8. Changes to Estimated Minimum Discharges of the SWDs

		Estimated Minimum Discharge ($m^3\ s^{-1}$)		
SWD	Reach/River	Surveyed Cross Section	Reduced Cross Section	% Reduction in Discharge
1A1	Barambah Creek	9000	8000	11
1B1	Barambah Creek	9000	7600	16
2A1	Mary River	6750	5400	19
2B1	Mary River	3800	2400	37
2B2	Mary River	3700	2250	39

example, the 2011 flood at the Spring Bluff gauge (14219A) in Lockyer Creek, in SEQ was originally estimated as a 1 in 2000 year flood (0.05% AEP) [*Rogencamp and Barton*, 2012]. However, the inclusion of two recent floods (2011 and 2013) into the AMS resulted in a revised ARI of 55 years for the 2011 flood [*Sargood et al.*, 2015]. However, in some cases, short flood records may also contain an overrepresentation of extreme floods [*Lam et al.*, 2016]. This is exemplified in Site 2, where the inclusion of five high magnitude floods in the short 85 year period immediately prior to the gauge records resulted in an increase in the estimated discharge of the 1% AEP (i.e., a decrease in the return period of a high magnitude flood). This reflects a scenario where too many high magnitude floods, over a relatively short record period, can create bias in FFA.

The temporal extension of flood records through the integration of historical and paleoflood records provides a means for improvement to FFA. Yet there remains reluctance to embrace the inclusion of such information and it is often founded in concerns about the inherent uncertainties associated with changing boundary conditions and more broadly the paleoflood discharges. Early paleoflood research, for example, focused almost exclusively on bedrock-walled channels which are assumed to experience limited changes

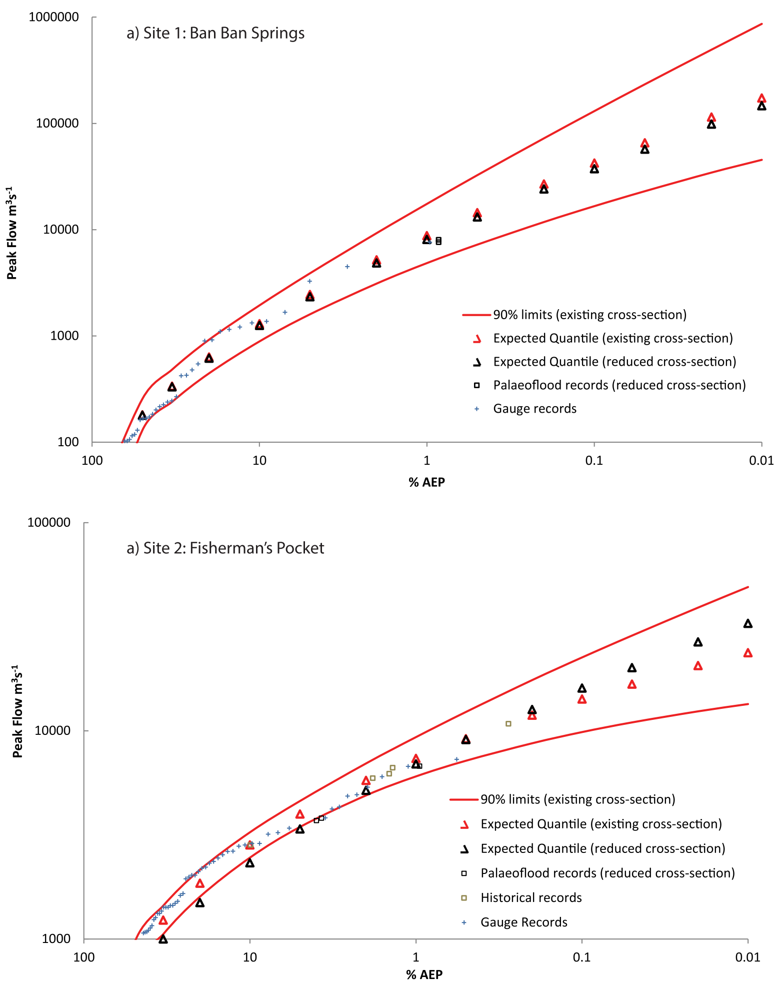

Figure 5. Estimated discharge quantile (with reduced cross-sectional area) relative to current estimated discharge quantile and 90% probability limits for Sites 1 and 2.

Table 9. Application of Existing Paleoflood Records to FFA in Other Locations in Australia

River	Source	Gauging Station	No. of Paleoflood Records Used	Estimated Minimum Discharge ($m^3 s^{-1}$)	Probability Distribution Model	Uncertainty Range Reduction (%)
Margaret	*Wohl et al.* [1994a]	802198	1	5,000	LPIII	58
Fitzroy	*Wohl et al.* [1994a]	802055	1	10,000	LPIII	60
Herbert	*Wohl* [1992]	116004ABC	5	10,000	LPIII	66

in cross-sectional capacity over time [*Webb and Jarrett*, 2002]. However, the restricted distribution of bedrock gorges often limits the application of paleoflood analysis in many parts of the world. The sensitivity analysis conducted to evaluate the effects of channel boundary changes in this study, provides confidence on the use of incorporating historical and paleoflood data with systematic gauge records to improve flood frequency estimates in a more widespread physical setting. The improved FFA results provide better information in a wide range of water-resources investigations and applications. The macrochannel morphology tends to be associated with regions of high hydrological variability [*Croke et al.*, 2013] and have been shown here to be a useful setting for further exploration of paleoflood studies.

Other uncertainties associated with the integration of paleoflood and historical flood records with gauge records include: (i) SWD preservation; (ii) OSL dating resolution; (iii) 1-D flow modeling; and (iv) reconstruction of paleoflood magnitudes. Although there is much concern about the completeness of the stratigraphic record in wide alluvial settings [*Sadler*, 1981], it is well established that slack-water zones are the optimum location for the preservation and accumulation of paleoflood deposits [*Baker*, 1987]. This is routinely supported by accompanying stratigraphical information which may indicate between-flood erosion or flood unit removal. In this study, the stratigraphy of the SWDs sampled showed no erosional contact layers and the record is assumed to be reasonably well preserved. However we cannot discount the occurrence of a flood which removed past SWD. The other concern is that the application of the SWD approach only records sediments of greater magnitude floods and hence does not provide a complete flood record. The Bayesian Inference approach circumvents this issue by working with additional information (i.e., historical and paleoflood records) rather than "complete" information.

Uncertainties in the hydraulic modeling were minimized at the study sites by using sites in close proximity to streamflow-gauging stations. The presence of debris lines and stage height information from land owners provided further means to improve the calibration of flow hydraulic modeling. The underestimation of the paleoflood discharge can result from the use of the depth of deposition as the stage height and has been shown to range between 9 and 20% [e.g., *Kochel et al.*, 1982; *Ely and Baker*, 1985; *Erskine and Peacock*, 2002]. The use of a minimum threshold value as the paleoflood discharge in FLIKE partly addresses this concern and reduces some of the uncertainties of a 1-D hydraulic model.

5.1. Improving Flood Frequency Analysis

Increasing attention has been given to developing alternative measures to improve uncertainty in flood frequency projection. The science of paleoflood hydrology is well established and growing global databases are increasingly recognized as an essential contribution to improved flood prediction. For example, *Sheffer et al.* [2003] compared the upper tail extrapolation of FFA before and after the incorporation of paleoflood and historical flood records in the Ardèche River, France. *Greenbaum et al.* [2014] integrated paleoflood records from the Colorado River into FFA and noted that the probable maximum flood (PMF) had a recurrence interval of 1000 years and that the use of only gauged records underestimates the frequencies of extreme floods. *Wasson* [2016] also argues that including paleoflood and historical data reduces aleatory uncertainty through improved statistical analyses. In this study, we sought to quantify the change (or improvement) to the FFA of the expected discharge estimate of the 1% AEP flood. The integration of historical and/or paleoflood records in this study also shows that changes to the return period of high magnitude floods occurs with the use of additional data and importantly, reduces uncertainty in the estimated discharge of the AEPs. In contrast, the integration of paleoflood records across all the sites showed a reduction in the discharge estimates for all return periods. This reflects a lack of extreme floods in the short gauging records and translates to an overestimation of the design flood's discharge, one typically used for risk assessment and planning. The reduction in the range of the 90% limits of all AEPs across all three sites provides greater confidence in the use of FFA for flood forecasting.

Despite being recommended in the national guidelines for flood design, such as in ARR [*Kuczera and Frank*, 2016], these additional sources of flood data are not routinely used. It is often incorrectly assumed, for example, that paleoflood studies require large numbers of samples and this is used to prevent the widespread implementation of the approach. On the contrary, this study highlights the significant contribution of relatively few paleoflood records into FFA in Australia and provides a clear justification for the inclusion of this methodology in subsequent flood predictions.

In Australia and other regions, where historical records are short, the significance of paleoflood records in improving FFA becomes more urgent. Paleoflood studies provide data to extend short gauged records and improve regional understanding of flood frequency. For area with limited gauge records, paleoflood studies can provide information on large floods at a fraction of the cost and time of adding new gauges and waiting decades for data. While the number of studies reporting the beneficial effects of extending the flood record, both through historical and paleoflood data, has increased, there remains some resistance to the adoption of this approach within the hydrological community. Much of this resistance reflects concerns regarding (1) nonsystematic data and (2) nonhomogeneous data [*Benito et al*., 2004]. The first issue is dealt with by using the Bayesian Inference approach. The latter, associated with climate and land use change, is an increasing concern as noted in the recent literature [e.g., *Milly et al*., 2008; *Ishak et al*., 2013; *Yu et al*., 2015]. *Greenbaum et al*. [2014] argued that using only short gauging records assumes stationarity in climate into the future. Therefore, the issues of climate change and land use change are not only limited to historical and paleoflood data, but are relevant to *all* flood data. The extent of nonstationarity in climate remains to be better understood. Nonetheless, to avoid significant implications of a different climate regime in the past, a conservative approach to exclude paleoflood data from more than ~1000 years ago was adopted in this study.

6. Conclusions

The inclusion of historical and paleoflood records with gauge records for at-site FFA significantly reduces the uncertainty associated with the estimated quantile of a given flood magnitude. The Bayesian Inference methodology used in this study is flexible enough to incorporate paleoflood records into FFA and even limited data makes a significant contribution to flood frequency prediction and increases confidence in flood risk management and planning in this region.

This study also highlights that the approach should not be limited by the availability of bedrock gorge sites. Sensitivity analysis shows that FFA is not significantly affected by within-channel boundary changes in confined semialluvial channels used in this study. Hence, these channel settings increase the potential range of sites for paleoflood reconstruction. This study provides a foundation to promote the incorporation of paleoflood hydrology for water-related issues (e.g., flood risk mapping) by engineers, planners, and managers.

Acknowledgments
This research was funded by an Australian Research Council Linkage Award (LP120200093). D.L. is supported by a University of Queensland (UQ) International Postgraduate Award Scholarship. Tim Pietsch, Wout Pulles, Pim van den Berg, and Robert Valkenburg are thanked for their field assistance. The landowners are thanked for providing access and ground information. John Vitkovsky is thanked for his verification of statistical result. We are grateful for the constructive comments by the Bob Jarrett and two other reviewers. Data used for the analyses presented here will be made available upon request.

References

Aitken, M. J. (1998), *Introduction to Optical Dating: The Dating of Quaternary Sediments by the Use of Photon-Stimulated Luminescence*, Clarendon, Oxford.

Australian Government (2015), *Natural Disasters in Australia*. [Available at http://www.australia.gov.au/about-australia/australian-story/natural-disasters.]

Baker, V. R. (1987), Palaeoflood hydrology and extraordinary flood events, *J. Hydrol*., *96*(1), 79–99.

Baker, V. R. (2008), Palaeoflood hydrology: Origin, progress, prospects, *Geomorphology*, *101*(1), 1–13.

Baker, V. R., and G. Pickup (1987), Flood geomorphology of the Katherine Gorge, northern territory, Australia, *Geol. Soc. Am. Bull*., *98*(6), 635–646.

Benito, G., and A. Díez-Herrero (2015), Palaeoflood hydrology: Reconstructing rare events and extreme flood discharges, in *Hydro- Meteorological Hazards, Risks, and Disasters*, edited by P. Paron, and G. Di Baldassarre, pp. 65–103, Elsevier, Amsterdam.

Benito, G., et al. (2004), Use of systematic, palaeoflood and historical data for the improvement of flood risk estimation. Review of scientific methods, *Nat. Hazards*, *31*(3), 623–643.

Benito, G., R. Brázdil, J. Herget, and M. J. Machado (2015), Quantitative historical hydrology in Europe, *Hydrol. Earth Syst. Sci*., *19*(8), 3517–3539.

Blewett, R. S., B. L. N. Kennett, and D. L. Huston (2012), Australia in time and space, in *Shaping a Nation: A Geology of Australia*, edited by R. S. Blewett, pp. 47–117, Geosci. Aust. and ANU E Press, Canberra.

Brázdil, R., Z. W. Kundzewicz, and G. Benito (2006), Historical hydrology for studying flood risk in Europe, *Hydrol. Sci. J*., *51*(5), 739–764.

Capelin, M., P. Kohn, and P. Hoffenberg (1998), Land use, land cover and land degradation in the catchment of Moreton Bay, in *Moreton Bay and Catchment*, edited by I. R. Tibbetts, N. J. Hall, and W. C. Dennison, pp. 55–66, Sch. of Mar. Sci., Univ. of Queensland, Brisbane, Australia.

Centre for Research on the Epidemiology of Disasters (2015), *The Human Coast of Weather-Related Disasters 1995-2015, UN International Strategy for Disaster Reduction (UNISDR)*, Geneva. [Available at http://www.unisdr.org/2015/docs/climatechange/COP21_WeatherDisastersReport_2015_FINAL.pdf.]

Croke, J., I. Reinfelds, C. Thompson, and E. Roper (2013), Macrochannels and their significance for flood-risk minimisation: Examples from southeast Queensland and New South Wales, Australia, *Stochastic Environ. Res. Risk Assess.*, *28*(1), 99–112.

Croke, J., C. Thompson, R. Denham, H. Haines, A. Sharma, and T. Pietsch (2016), Reconstructing a millennial-scale record of flooding in a single valley setting: The 2011 flood-affected Lockyer Valley, south-east Queensland, Australia, *J. Quat. Sci.*, *31*(8), 936–952.

Daley, J. S., J. C. Croke, C. J. Thomspon, T. J. Cohen, M. Macklin, and A. Sharma (2017), Late Quaternary channel and floodplain formation in a partly confined subtropical river, Eastern Australia, *J. Quat. Sci.*, in press, doi:10.1002/jqs.2930.

Ely, L. L., and V. R. Baker (1985), Reconstructing palaeoflood hydrology with slackwater deposits: Verde River, Arizona, *Phys. Geogr.*, *6*(2), 103–126.

Erskine, W. D., and C. T. Peacock (2002), Late Holocene flood plain development following a cataclysmic flood, *Int. Assoc. Hydrol. Sci.*, *276*, 177–184.

Fryirs, K., P. Lisenby, and J. Croke (2015), Morphological and historical resilience to catastrophic flooding: The case of Lockyer Creek, SE Queensland, Australia, *Geomorphology*, *241*, 55–71.

Galbraith, R. F., and G. M. Laslett (1993), Statistical models for mixed fission track ages, *Nucl. Tracks Radiat. Meas.*, *21*(4), 459–470.

Galbraith, R. F., R. G. Roberts, G. M. Laslett, H. Yoshida, and J. M. Olley (1999), Optical dating of single and multiple grains of quartz from Jinmium rock shelter, northern Australia: Part I, experimental design and statistical models, *Archaeometry*, *41*(2), 339–364.

Gillieson, D., D. I. Smith, M. Greenaway, and M. Ellaway (1991), Flood history of the limestone ranges in the Kimberley region, Western Australia, *Appl. Geogr.*, *11*(2), 105–123.

Greenbaum, N., T. M. Harden, V. R. Baker, J. Weisheit, M. L. Cline, N. Porat, R. Halevi, and J. Dohrenwend (2014), A 2000 year natural record of magnitudes and frequencies for the largest Upper Colorado River floods near Moab, Utah, *Water Resour. Res.*, *50*, 5249–5269, doi: 10.1002/2013WR014835.

Harden, T., M. G. Macklin, and V.R. Baker (2010), Holocene flood histories in south-western USA, *Earth Surf. Processes Landforms*, *35*(6), 707–716.

Heitmuller, F. T., P. F. Hudson, and W. H. Asquith (2015), Lithologic and hydrologic controls of mixed alluvial–bedrock channels in flood-prone fluvial systems: Bankfull and macrochannels in the Llano River watershed, central Texas, USA, *Geomorphology*, *232*, 1–19.

Herget, J., and H. Meurs (2010), Reconstructing peak discharges for historic flood levels in the city of Cologne, Germany, *Global Planet. Change*, *70*(1), 108–116.

Heritage, G. L., B. P. Moon, G. P. Jewitt, A. R. G. Large, and M. Rountree (2001), The February 2000 floods on the Sabie River, South Africa: An examination of their magnitude and frequency, *Koedoe*, *44*(1), 37–44.

Hogg, A. G., et al. (2013), SHCal13 Southern Hemisphere calibration, 0–50,000 years cal BP, *Radiocarbon*, *55*(2), 1–15.

Ishak, E. H., A. Rahman, S. Westra, A. Sharma, and G. Kuczera (2013), Evaluating the non-stationarity of Australian annual maximum flood, *J. Hydrol.*, *494*, 134–145.

Jarrett, R. D., and J. F. England (2002), Reliability of paleostage indicators for paleoflood studies, in *Ancient Floods, Modern Hazards: Principles and Applications of Palaeoflood Hydrology, Water Science and Application*, vol. 5, edited by P. K. House et al., pp. 91–109, AGU, Washington, D. C.

Kochel, R. C., V. R. Baker, and P.C. Patton (1982), Paleohydrology of southwestern Texas, *Water Resour. Res.*, *18*(4), 1165–1183.

Kuczera, G. (1999), Comprehensive at-site flood frequency analysis using Monte Carlo Bayesian Inference, *Water Resour. Res.*, *35*(5), 1551–1557, doi:10.1029/1999WR900012.

Kuczera, G., and S. Frank (2016), At-site flood frequency analysis, in *Australian Rainfall and Runoff: A Guide to Flood Estimation, Book 3*, edited by J. Ball et al., Commonw. Aust.

Lam, D., C. Thompson, and J. Croke (2016), Improving at-site flood frequency analysis with additional spatial information: A probabilistic regional envelope curve approach, *Stochastic Environ. Res. Risk Assess.*, 1–21, doi:10.1007/s00477-016-1303-x.

Lamontagne, J. R., J. R. Stedinger, X. Yu, C. A. Whealton, and Z. Xu (2016), Robust flood frequency analysis: Performance of EMA with multiple Grubbs-Beck outlier tests, *Water Resour. Res.*, *52*, 3068–3084, doi:10.1002/2015WR018093.

Machado, M. J., B. A. Botero, J. López, F. Francés, A. Díez-Herrero, and G. Benito (2015), Flood frequency analysis of historical flood data under stationary and non-stationary modelling, *Hydrol. Earth Syst. Sci.*, *19*, 2561–2576.

Macklin, M. G., and J. Lewin (2003), River sediments, great floods and centennial-scale Holocene climate change, *J. Quat. Sci.*, *18*(2), 101–105.

Merz, R., and G. Blöschl (2008), Flood frequency hydrology: 1. Temporal, spatial, and causal expansion of information, *Water Resour. Res.*, *44*, W08432, doi:10.1029/2007WR006744.

Milly, P. C. D., B. Julio, F. Malin, M. Robert, W. Zbigniew, P. Dennis, and J. Ronald (2008), Stationarity is dead: Whither water management?, *Science*, *319*(5863), 573–574.

Olley, J. M., T. Pietsch, and R. G. Roberts (2004), Optical dating of Holocene sediments from a variety of geomorphic settings using single grains of quartz, *Geomorphology*, *60*(3), 337–358.

Parkes, B., and D. Demeritt (2016), Defining the hundred year flood: A Bayesian approach for using historic data to reduce uncertainty in flood frequency estimates, *J. Hydrol.*, *540*, 1189–1208.

Pickup, G., G. Allan, and V. Baker (1988), History, paleochannels and palaeofloods of the Finke river, Central Australia, in *Fluvial Geomorphology of Australia*, edited by R. F. Warner, pp. 177–200, Academic, Sydney, N. S. W., Australia.

Pietsch, T. J. (2009), Optically stimulated luminescence dating of young (<500 years old) sediments: Testing estimates of burial dose, *Quat. Geochronol.*, *4*(5), 406–422.

Pointon, S. M., and A. W. Collins (2000), *Mary River Catchment Resource Atlas*, Dep. of Nat. Resour., Queensland, Australia.

Queensland Floods Commission of Inquiry (2012), *Chapter 14: Flood-Related Deaths*. [Available at http://www.floodcommission.qld.gov.au/publications/final-report/.]

Rahman, A. S., K. Haddad, and A. Rahman (2014), Impacts of outliers in flood frequency analysis: A case study for Eastern Australia, *J. Hydrol. Environ. Res.*, *2*(1), 17–13.

Roberts, R. G., R. F. Galbraith, H. Yoshida, G. M. Laslett, and J. M. Olley (2000), Distinguishing dose populations in sediment mixtures: A test of single-grain optical dating procedures using mixtures of laboratory-dosed quartz, *Radiat. Meas.*, *32*(5), 459–465.

Rogencamp, G., and J. Barton (2012), The Lockyer Creek flood of January 2011: What happened and how should we manage hazard for rare floods, paper presented at 52nd Annual Floodplain Management Association Conference, Newcastle, NSW, Australia. [Available at http://www.floodplainconference.com/papers2012.php.]

Rustomji, P., N. Bennett, and F. Chiew (2009), Flood variability east of Australia's great dividing range, *J. Hydrol.*, *374*(3), 196–208.

Sadler, P. M. (1981), Sediment accumulation rates and the completeness of stratigraphic sections, *J. Geol.*, *89*, 569–584.

Sargood, M. B., T. J. Cohen, C. J. Thompson, and J. Croke (2015), Hitting rock bottom: Morphological responses of bedrock-confined streams to a catastrophic flood, *Earth Surf. Dyn.*, *3*(2), 265–279.

Saynor, M. J., and W. D. Erskine (1993), Characteristics and implications of high-level slackwater deposits in the Fairlight Gorge, Nepean River, *Australia*, *Mar. Freshwater Res.*, *44*(5), 735–747.

Sheffer, N. A., Y. Enzel, G. Benito, T. Grodek, N. Poart, M. Lang, R. Naulet, and D. Coeur (2003), Palaeofloods and historical floods of the Ardèche River, France, *Water Resour. Res.*, *39*(12), 1376, doi:10.1029/2003WR002468.

Swain, R. E., J. F. England Jr., K. L. Bullard, and D. A. Raff (2004), Hydrologic hazard curve estimating procedures, *Dam Safety Res. Program Res. Rep. DSO-04-08*, U.S. Dep. of Inter., Bur. of Reclam., Denver, Colo.

Talma, A. S., and J. C. Vogel (1993), A simplified approach to calibrating (super 14) C dates. *Radiocarbon*, *35*(2), 317–322.

Thompson, C., and J. Croke (2013), Geomorphic effects, flood power, and channel competence of a catastrophic flood in confined and unconfined reaches of the upper Lockyer valley, southeast Queensland, Australia, *Geomorphology*, *197*, 156–169.

Thompson, C. J., J. Croke, K. Fryirs, and J. R. Grove (2016), A channel evolution model for subtropical macrochannel systems, *Catena*, *139*, 199–213.

Thorndycraft, V. R., and G. Benito (2006), Late Holocene fluvial chronology of Spain: The role of climatic variability and human impact, *Catena*, *66*(1), 34–41.

Wasson, R. J. (2016), Uncertainty, ambiguity and adaptive flood forecasting, *Policy Soc.*, *35*, 125–136, doi:10.1016/j.polsoc.2016.06.002.

Webb, R. H., and R. D. Jarrett (2002), One-dimensional estimation techniques for discharges of paleofloods and historical floods, in *Ancient Floods, Modern Hazards: Principles and Applications of Palaeoflood Hydrology, Water Science and Application*, vol. 5, edited by P. K. House et al., pp. 111–125, AGU, Washington, D. C.

Webb, R. H., J. B. Blainey, and D. W. Hyndman (2002), Palaeoflood hydrology of the Paria River, southern Utah and northern Arizona, USA, in *Ancient Floods, Modern Hazards: Principles and Applications of Palaeoflood Hydrology, Water Science and Application*, vol. 5, edited by P. K. House et al., pp. 295–310, AGU, Washington, D. C.

Willmott, W. F. (1986), *1986 Field Conference South Burnett District*, Geol. Soc. of Austr., Queensland Div., Queensland.

Wohl, E. E. (1992), Bedrock benches and boulder bars: Floods in the Burdekin Gorge of Australia, *Geol. Soc. Am. Bull.*, *104*(6), 770–778.

Wohl, E. E., S. J. Fuertsch, and V. R. Baker (1994a), Sedimentary records of late Holocene floods along the Fitzroy and Margaret Rivers, Western Australia, *Aust. J. Earth Sci.*, *41*(3), 273–280.

Wohl, E. E., R. H. Webb, V. R. Baker, and G. Pickup (1994b), *Sedimentary Flood Records in the Bedrock Canyons of Rivers in the Monsoonal Region of Australia. Water Resources Papers*, vol. 107, Colo. State Univ., Ft. Collins.

Woodward, C., J. Shulmeister, D. Bell, R. Haworth, G. Jacobsen, and A. Zawadzki (2014), A Holocene record of climate and hydrological changes from Little Llangothlin Lagoon, south Eastern Australia, *Holocene*, *24*, 1–10, doi:10.1177/0959683614551218.

Yu, X., T. A. Cohn, and J. R. Stedinger (2015), Flood frequency analysis in the context of climate change, in *World Environmental and Water Resources Congress*, edited by K. Karvazy and V. Webster, pp. 2376–2385, Am. Soc. of Civ. Eng.